ENVIRONMENTAL ENGINEERING

The 8th International Conference
May 19–20, 2011, Vilnius, Lithuania
Selected papers

ISSN 2029-7106 print / ISSN 2029-7092 online
ISBN 978-9955-28-826-8 (1 Volume)
ISBN 978-9955-28-827-5 (3 Volumes)
http://enviro.vgtu.lt

EVALUATION OF OZONE BEHAVIOR IN A COMPLEX COASTAL ENVIRONMENT

Giorgio Passerini[1], Giancarlo Ciarelli[2], Stefano Carletti[3]

[1, 2, 3]*Università Politecnica delle Marche, Via Brecce Bianche 60131 Ancona, Italy.*
E-mail: [1]g.passerini@univpm.it

Abstract. Aim of this work is to evaluate the ozone dynamics in a coastal region on the Adriatic Sea that is under the "High Environmental Risk Area" restraint. By the implementation of a particular tool called OSAT (Ozone Source Apportionment Technology) into the photochemical model CAMx (Comprehensive Air quality Model with eXtensions), it was possible to discriminate between NOx-limited and VOC-limited condition formation. Information about the contribution of the different types of source emission-groups, allowed us to develop a tentative best ozone-control strategy to lower ozone peaks and to avoid ozone episodes. Particular emphasis was given to the study of initial and boundary conditions in order to discover how they affect the final solution. Various extensions of domain were tested with the aim of finding the choice one. The study includes comparison between several concentration data sets related to different species (e.g. NO, NO_2, VOC, O_3) given as results by the photochemical model (under certain meteorological, orographic and emission data) and the concentrations recorded at monitoring stations at various locations. It was also possible to analyze the ozone behavior in diverse areas based on land use (e.g. Road, Country, Industrial Area, Etc.). Finally, new simulation scenarios, with reduction of chemicals in specific emission groups, were launched to analyze the ozone response.

Keywords: air pollution, ozone, VOC, NOx, OSAT, CAMx, air control strategies.

1. Introduction

This paper presents a rather complex set of simulations carried out to better describe the ozone behavior in a particular area located across the Adriatic Sea in the Marche region that is under the "High Environmental Risk Area" restraint. The risk is mainly due to the concurrent presence of a big oil refinery, several highways, the local airport, and a rather big port, including industrial harbors. This led, in the past, to high levels of several different species of pollutants (especially Volatile Organic Compounds) many of whom deeply affect ozone cycles. In past years, comparatively high concentrations of ozone were registered by monitoring stations even during the night, while the ozone level decreases to zero only in the very early morning.

The entire "Ozone Problem" in such area was modeled by the means of the photochemical model CAMx (Comprehensive Air quality Model with eXtensions) with the additional implementation of a dedicated probing tool called OSAT (Ozone Source Apportionment Technology) specially developed for the study of the ozone dynamics.

The results provided us with important information about the conditions of ozone formation, the role of each single emission group, and, more specifically, information about when and where a certain pollutant involved in the ozone dynamics were released.

2. CAMx and the probing tool OSAT

CAMx is an Eulerian photochemical dispersion model that allows an integrated "one-atmosphere" assessment of gaseous and particulate air pollution (ozone, PM2.5, PM10, air toxics, mercury) over many scales ranging from sub-urban to continental.

CAMx simulates the emission, dispersion, chemical reaction, and removal of pollutants in the troposphere by solving the pollutant continuity equation for each chemical species on a system of nested three-dimensional grids. The Eulerian continuity equation describes the time dependency of the average species concentration within each grid-cell volume as a sum of all of the physical and chemical processes operating on that volume.

CAMx can perform simulations on three types of Cartesian map projections: Universal Transverse Mercator, Rotated Polar Stereographic, and Lambert Conic Conformal. CAMx also offers the option of operating on a curve-linear geodetic latitude/longitude grid system as well.

Furthermore, the vertical grid structure is characterized externally, so layer interface heights may be given as any arbitrary function of space and/or time. This flexibility in defining the horizontal and vertical grid structures allows CAMx to be configured to match the grid of any meteorological model used to provide environmental input

fields. For this purpose, we employed the Regional Air Modeling System, RAMS (Walko and Tremback 2006).

Another tool, namely OSAT, allows CAMx to track source-region and source-category contributions to the predicted ozone concentrations. Thus, for any selected receptor and for any selected period, the model gives information of the likely distribution of ozone and ozone precursors by source category and by source region, as well as an indication as to whether the ozone at the selected time and location would more likely respond to upwind NOx or VOC controls.

OSAT uses multiple tracer-species to track the fate of ozone precursor emissions (VOC and NOx) and the ozone formation caused by these emissions within a simulation. The tracers operate as spectators to the normal CAMx calculations so that the underlying CAMx predicted relationships between emission groups (sources) and ozone concentrations at specific locations (receptors) are not perturbed. Tracers of this type are conventionally referred to as "passive tracers" but it is important to realize that the tracers in the OSAT track the effects of chemical reaction, transport, diffusion, emissions and deposition within CAMx so that they are described as "ozone reaction tracers". The ozone reaction tracers allow ozone formation from multiple "source groupings" to be tracked simultaneously within a single simulation. A source grouping can be defined in terms of geographical area and emission category (Morris *et al.* 2001). CAMx boundary conditions and initial conditions are always tracked as separate source groupings.

In addition to using ozone reaction tracers to apportion ozone formation, the OSAT uses separate families of timing tracers to allow source-receptor transport times to be estimated. Unique timing tracers are released from each geographical area selected for ozone-source apportionment. Thus, if the ozone formation tracers show that emissions from a given source area contributed to ozone at any receptor of interest, the timing tracers can then be used to estimate the time at which the emissions were released. This provides a method for investigating temporal behavior of source-receptor relationships and for developing time-biased control strategies.

3. Ozone Formation the VOC/NOx Role and the Sillman Indicator

The hydroxyl radical is the key reactive species in the chemistry of ozone formation. The VOC-OH reaction initiates the oxidation sequence. There is a competition between VOCs and NOx for the OH radical. At a high ratio of VOC to NOx concentration, OH will react mainly with VOCs while at a low ratio, the NOx reaction can predominate. Hydroxyl reacts with VOC and NO_2 at an equal rate when the VOC/NO_2 concentration ratio is a certain value that depends on the particular VOC or mix of VOCs present, as the OH rate constants of VOCs differ for each VOC species. At ambient conditions the second-order rate constant for the OH+NO_2 reaction is, in mixing ratio units, approximately 1.7×10^4 ppm^{-1} min^{-1}. Considering an average urban mix of VOCs, an average VOC-OH rate constant, expressed on a per-carbon-atom basis, is about 3.1×10^3 ppm C^{-1} min^{-1}. Using this value for an average VOC-OH rate constant, the ratio of the OH-NO_2 to OH-VOC rate constants is about 5.5. Thus, when the VOC/NO_2 concentration ratio is approximately 5.5:1, with the VOC concentration expressed on a carbon atom basis, the rates of reaction of VOC and NO_2 with OH are equal. Whenever the VOC/NO_2 ratio is lower than 5.5:1, reaction of OH with NO_2 predominates over reaction of OH with VOCs. The OH-NO_2 reaction removes OH radicals from the active VOC oxidation cycle, retarding the further production of O_3. On the other hand, when the ratio exceeds 5.5:1, OH reacts preferentially with VOCs. At a minimum, no new radicals are produced or destroyed but photolysis of intermediate products generated by the OH-VOC reactions generates new radicals, accelerating O_3 production (Barker 1995).

NOx tends to be removed from a certain mixture of VOCs and NOx faster than VOCs since OH reacts about 5.5 times more quickly with NO_2 than with VOCs. As the system evolve without new NOx emissions, NOx are depleted more rapidly than VOCs, and the local VOC:NO_2 ratio will increase with time. The concentration of NOx may become sufficiently low because of the continual removal of NOx by the OH-NO_2 reaction that OH reacts preferentially with VOCs to keep the ozone-forming cycle going. At very low NOx concentrations, peroxy radical to peroxy radical reactions begin to become important (Seinfeld and Spyros 2006).

A classic trajectory model, the EKMA diagram, can be used to distinguish VOC-limited from NOx-limited trajectories and to develop a classification based on initial VOC-to-NOx ratio. However, this approach classifies VOC-limited or NOx- behavior on the response of peak ozone, which is the net response from several hours of photochemistry. In fact, many of the trajectories begin as VOC-limited and become NOx-limited during the course of the day essentially for the reason that the NOx is depleted more rapidly than the VOC. For OSAT, a more fundamental indicator of the instantaneous state of ozone formation with regard to VOC or NOx-limitation is required.

Ozone formation occurs through the following sequence of reactions. The sequence is usually initiated by the reaction of various VOC or CO with the OH radical according to formulae (1) and (2).

$$VOC + OH \xrightarrow{O_2} RO_2 + H_2O \quad (1)$$

$$CO + OH \xrightarrow{O_2} HO_2 + CO_2 \quad (2)$$

This is followed by the conversion of NO to NO_2 through reaction with HO_2 or RO_2 radicals, which also regenerates OH according to formulae (3) and (4). RO_2 represents any of a number of chains of organics with an O_2 attached.

$$RO_2 + NO \longrightarrow VOC^* + HO_2 + NO_2 \quad (3)$$

$$HO_2 + NO \longrightarrow OH + NO_2 \quad (4)$$

NO_2 is photolyzed to generate atomic oxygen, which combines with O_2 to create O_3 through reaction (5) and (6).

$$NO_2 + h\nu \longrightarrow NO + O \quad (5)$$

$$O + O_2 + M \longrightarrow O_3 + M \quad (6)$$

The rate of ozone formation is controlled primarily by the rate of the initial reaction of VOC with OH.

Ozone episodes in polluted regions are usually due to the ozone production sequence shown above. However, at nighttime and in the immediate vicinity of very large emissions of NO, ozone concentrations are depressed through the process of NOx titration i.e. the O_3 removal through reaction with NO according to the formula:

$$NO + O_3 \longrightarrow NO_2 + O_2 \quad (7)$$

During the daytime, this reaction is normally balanced by the photolysis of NO_2 according to (5) and (6).

The sensitivity of ozone formation to VOCs and NOx at any given time is attributable to the fate of radicals. The radical pool is often referred to as odd hydrogen (HOx) and is most usefully considered as the sum of OH, HO_2 and RO_2 radicals.

When NOx is plentiful, the main radical termination, a.k.a. HOx removal, pathway is nitric acid formation through:

$$HO + NO_2 + M \longrightarrow HNO_3 + M \quad (8)$$

Under these conditions, ozone formation is limited by the rate at which radicals can be formed, which is generally described as the VOC-limited condition. Thus, nitric acid (HNO_3) production is indicative of plentiful NOx and VOC-limited ozone formation.

When NOx are scarce, radical-radical reactions dominate HOx removal, e.g.

$$HO_2 + HO_2 + M \longrightarrow H_2O_2 + O_2 + M \quad (9)$$

$$HO_2 + RO_2 + M \longrightarrow ROOH + O_2 \quad (10)$$

Under these conditions, ozone formation is limited by the availability of NO to react with HO_2 and RO_2 radicals, which is described as the NOx-limited condition. HO_2 and RO_2 radicals that do not react with NO participate in peroxide formation. Thus, the formation of hydrogen peroxide (H_2O_2) or organic hydro-peroxides (ROOH) is indicative of scarce NOx in NOx-limited ozone formation.

The production rates of nitric acid (P_{HNO3}) and hydrogen peroxide (P_{H2O2}) in each CAMx grid cell at each time step are available while the production rate of organic peroxides (P_{ROOH}) is not due to the CB4 mechanism that does not explicitly track these species (Dunker *et al.* 2002). The balance between P_{ROOH} and P_{H2O2} is governed by the comparative production of HO_2 and RO_2 radicals, and is not highly variable across simulations. Sillman proposes (Sillman *et al.* 1990; 1995; 1997; 2002) a transition point of

$$P_{H_2O_2} / P_{HNO_3} = 0.35 \quad (11)$$

In other words, when the above ratio exceeds 0.35, ozone formation is NOx-limited, and when this ratio is less than 0.35 ozone formation is VOC-limited.

4. Human Health Effects

The effects on human health of ozone have been studied for over 30 years. The respiratory system is the primary target of its oxidizing effects. Such effects include reduction in lung function and exasperation of original respiratory disease (e.g. asthma), which result into increased daily hospital admissions, emergency department visits for respiratory causes, and additional mortality (Cody *et al.* 1992).

The extent of adverse respiratory consequences due to ground-level ozone depends on a number of factors, including pollutant concentrations, duration of exposure, local climate, individual sensitivity, and any preexistent respiratory disease.

The Air Quality Index (AQI) is an indicator of the effects on human health due to certain levels of airborne pollutants developed in the framework of National Ambient Air Quality Standards (NAAQS). The AQI scale is split into ranges, which span from zero to 300.

Each step corresponds to a different health impact. The upper limits of NAAQS for ozone are 0.120ppb averaged over 1 hour and 0.08ppb averaged over 8 hours. At ozone concentrations from 0.125 to 0.404ppm, susceptible people experience severe respiratory symptoms so to impair breathing.

Surveys on humans exposed, during heavy exercise, to high ozone concentrations revealed pulmonary function impairment.

Other studies demonstrated that an hourly exposure at levels ranging from 0.170 to 0.250ppm statistically increases the occurrence of respiratory symptoms, such as cough, phlegm, and general difficulty in breathing. Hourly ozone exposure to higher concentrations induces lower airway inflammation.

5. Definition of the Domain

For the present study, we used three differed grids as shown in Fig 1, 2 and 3: one master grid (always required by the program) and two optional nested grids. The coarse grid (G1) is 960x800km wide and covers most of continental Italy through its 60x50 cells with 16km step. The second nested grid (G2) is 232x219Km wide, well covers the Marche region, and is made of 58x54 cells of 4 km steps.

The finest grid (G3) is 50x50km wide and is made of 50x50 cells of 1 km steps. It covers the "High Environmental Risk Area".

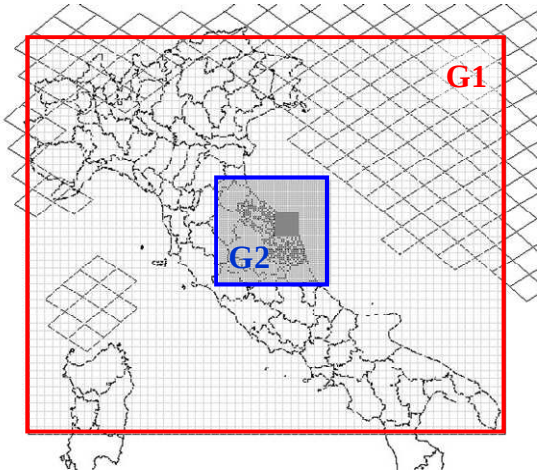

Fig 1. Master grid G1 and nested grid G2

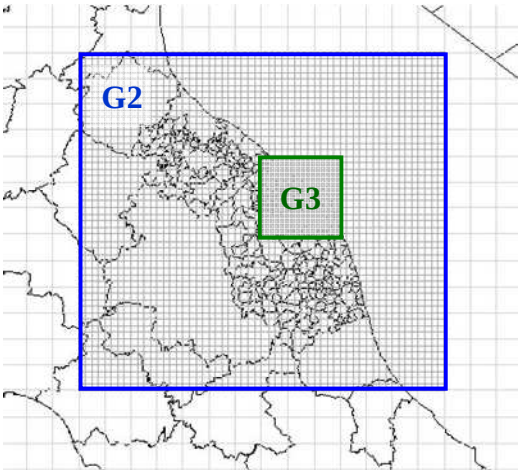

Fig 2. First nested grid G2 and finest grid G3

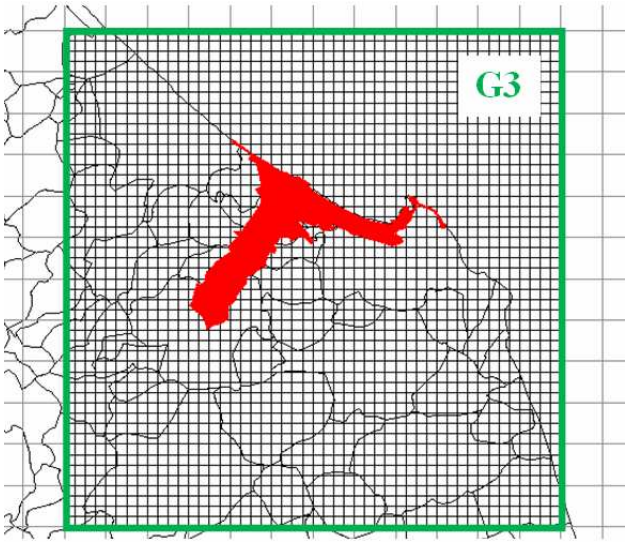

Fig 3. Grid G3 with High Environmental Risk Area (red)

6. Simulation Settings

Our preliminary study was performed over four days, namely from August 25 to August 28 of 2006.

The advection solver used for this simulation into the CAMx model was the Piecewise Parabolic Method. This scheme possesses high-order accuracy, little numerical diffusion, and is sufficiently quick for applications on very large grids.

For the chemistry solver, the Euler-Backward Iterative (EBI) model has replaced the original Chemistry Mechanism Compiler (CMC) employed in past versions of CAMx. EBI provides improved accuracy with similar speed compared to CMC.

Finally, the chemistry mechanisms activated was Carbon Bond IV (Gery *et al.*, 1989) with 113 reactions and up to 76 species (up to 44 state gases, up to 22 state particulates, and 10 radicals).

The emission data was roughly split into three different groups: Industry (001), Road (002) and Natural (003). The time-release option was activated into the CAMx control file in order to retrieve information about the epoch a pollutant was emitted.

The tool OSAT needs an input file called Source Map file that allows the user to indicate other subdomains of emission within the grid set before. A Source Map file is required for the master grid and optional for the nested ones. The Source Map, showed in Fig 4, was designed according to the borders of Italian Regions. Smaller Regions were joined together.

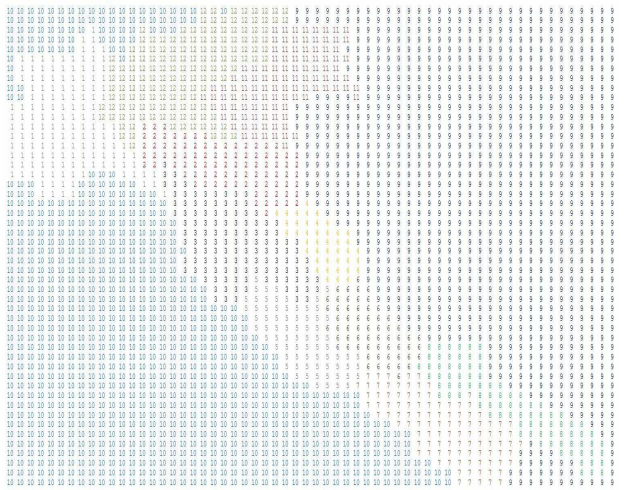

Fig 4. Source Map File, each number represents a Region

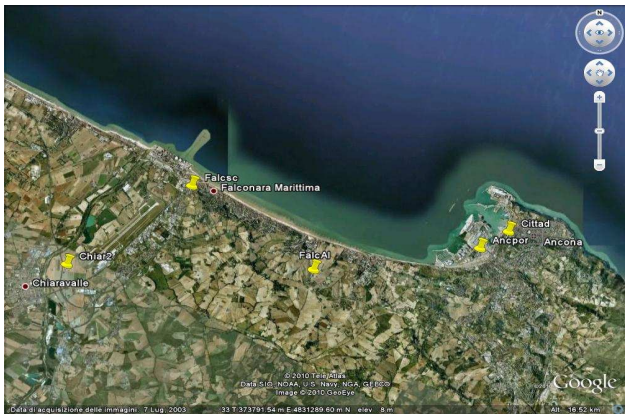

Fig 5. The location of official monitoring stations

The tool can now give in output the single contributions to the total ozone due to the three emission groups differentiated through the type of emission, and those due to other 12 emission groups differentiated based on the emission area. Finally, an input receptor file will indicate to CAMx the points on the grid where the concentration should be registered. Five different points were added to evaluate data at the sites of official monitoring stations.

7. Simulation analysis

To quantify the model response to the boundary conditions, several different simulations were launched to perform a sensitivity analysis and to conduct a first preliminary comparison with data monitored at stations.

The first simulation has no boundary condition so there is no flux of pollutant into the domain (Fig 6).

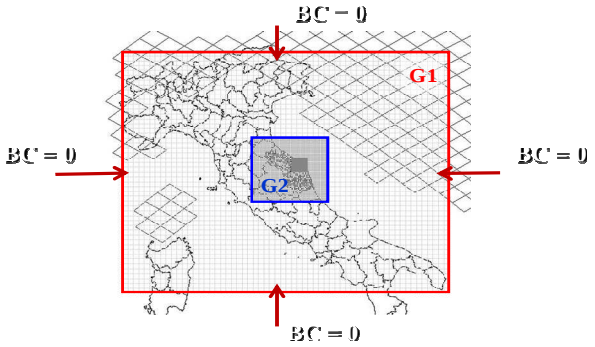

Fig 6. Outer boundary condition set to zero

Fig 7 and Fig 8 show hourly ozone concentrations predicted by CAMx (OSAT series) and the ones recorded at "Chiaravalle" monitoring station (Chiar2 series) on the 27 and 28 of August.

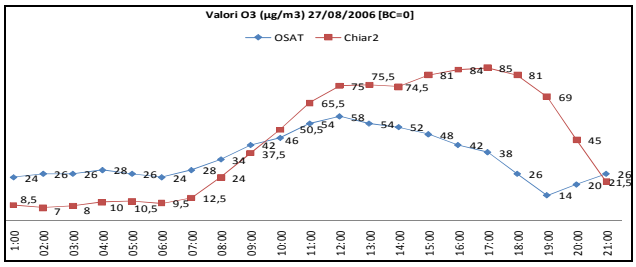

Fig 7. Results, with null boundary concentrations, on August 27 and monitored values at "Chiaravalle2" station

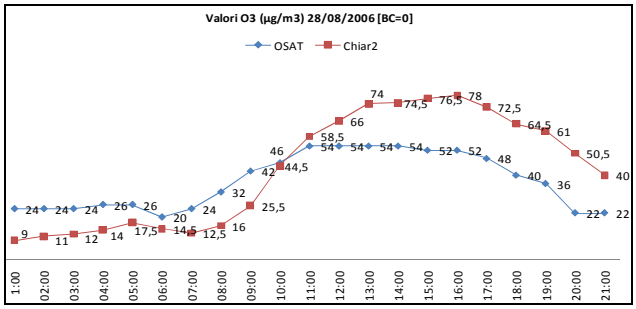

Fig 8. Results, with null boundary concentrations, on August 28 and monitored values at "Chiaravalle2" station

There is a good agreement between ozone levels predicted by the model and experimental data but the model tend to underestimate during peak hours to overestimate during the night. These differences become smaller on the 28 simply due to the further self-tuning of the model. This is also the reason for which the first two days 25th and 26th are not reported: the model need at least two days of simulation to give acceptable results.

The results of a second simulation, with non-null boundary conditions, are shown in Fig 9 and Fig 10. With new, non-null boundary conditions, evaluated from EMEP prescribed values and reports (EMEP 2003), the predicted concentration are in much better agreement with monitored values.

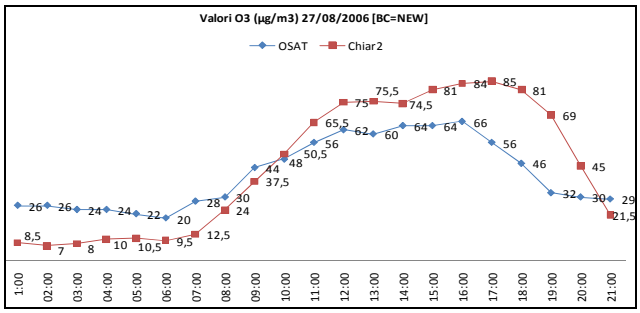

Fig 9. Results with EMEP boundary conc. on August 27

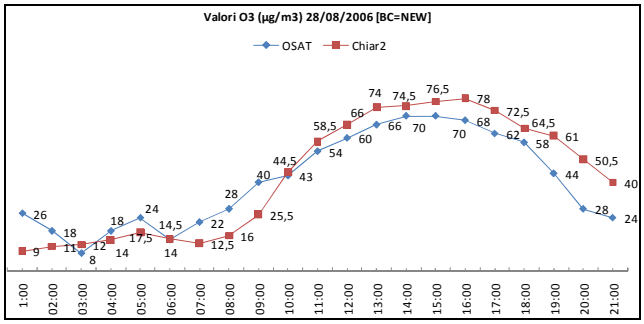

Fig 10. Results with EMEP boundary conc. on August 28

8. Ozone formation

In this paragraph, the detailed information regarding the ozone formation process evaluated by means of OSAT will be presented. The receptor analyzed is "Falconara Scuola", located very close to a rather big oil refinery, and, thus, more directly affected to changes of precursor emission rates. The Fig 11 shows the ozone behavior during the day at site.

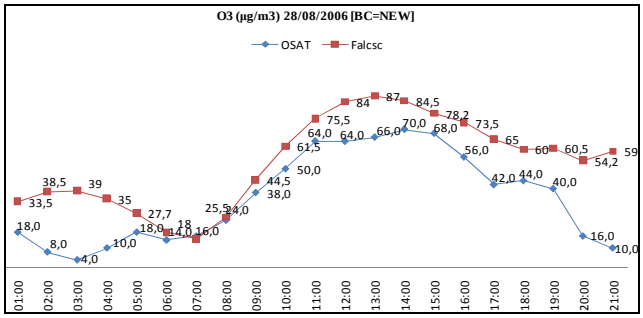

Fig 11. Results with EMEP boundary concentrations on August 28 at "Falconara Scuola" monitoring site

CAMx predicted an acceptable behavior of the ozone during the day. At night, the predicted ozone concentrations are close to zero while the monitoring station continues to register relatively high concentrations. In fact, we had already noticed this uncommon behavior of ozone during the night and we had already stated to focus on the point. The results in terms of contributions carried out by OSAT are visible in Table 1.

Table 1. Detailed contributions to ozone on Aug.28 at peak

Source location (Fig.4)	Sour-ceType Group	NOx-limited quota	VOC-limited quota	Total	Time-Emitted
IC				29%	
BC				27%	
3	002	4%	2%	6%	8/27 7PM
6	002	4%	2%	6%	8/27 8PM
4	002	4%	2%	6%	8/28 12PM
10	002	4%	0	4%	8/27 9AM
5	002	3%	1%	4%	8/27 4PM
10	001	3%	0	4%	8/27 9AM
3	001	2%	0	2%	8/27 7PM
5	001	1%	0	1%	8/27 4PM
3	003	0	1%	1%	8/27 7PM
7	002	1%	0	1%	8/26 5PM
6	001	1%	0	1%	8/27 8PM

The table 1 shows the contribution of each emission area defined in the source map file (see Fig. 4) and the contribution of each category of emission (e.g. 002=Roads). The initial condition refers to the amount of ozone formed at 11.59 PM of the 27, thus the day before. The analysis shows an important contribution (namely 27 %) due to the boundary conditions and a significant amount of ozone formed within the nearby areas (e.g. Area 3 counts for 6 %, Area 6 counts for 6 %).

The most important emission category for the ozone is “002”, which corresponds to “Roads” emission group.

The time-emitted column also gives information about when a certain precursor involved in the ozone formation is emitted. Precursors coming from a distant area are emitted several hours (or a day) before because of the time to travel, during the night, under certain meteorological conditions, so to reach the analyzed receptor.

The most important information regarding the conditions of formation is given in the VOC-limited and NOx-limited columns. Fig 12 shows the hourly amount of ozone formed with respect to the condition of formation for all emission groups and all emission areas. Fig 13 shows the Sillman indicator at the Falc. Scuola receptor.

During the first part of the morning, at high concentration of NOx, the reaction of the radical HOx is faster with NOx than with VOC and so the production of nitric acid, according to Formula (1), is high and the Sillman Indicator starts descending (VOC-limited situation). The transition happens at about 12:30 AM. At this point because of a low concentration of NOx, the radical HOx react faster with VOC, the radical-radical reaction (2) becomes predominant and the Sillman indicator starts increasing (NOx-limited situation).

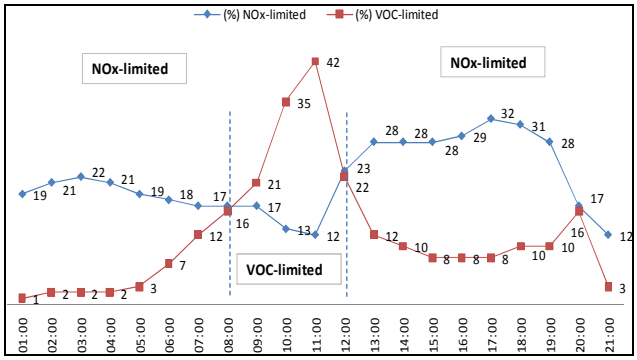

Fig 12. Ozone condition of formation during the day

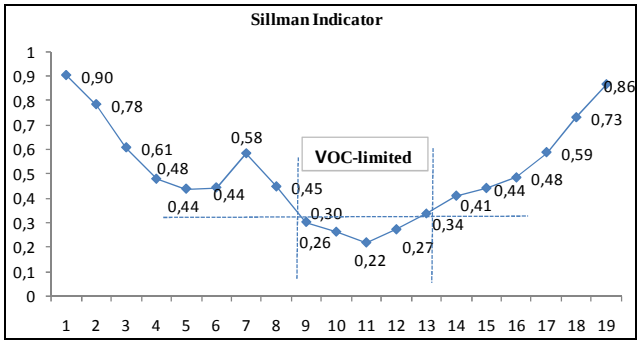

Fig 13. Sillman indicator during the day at Falc. Scuola

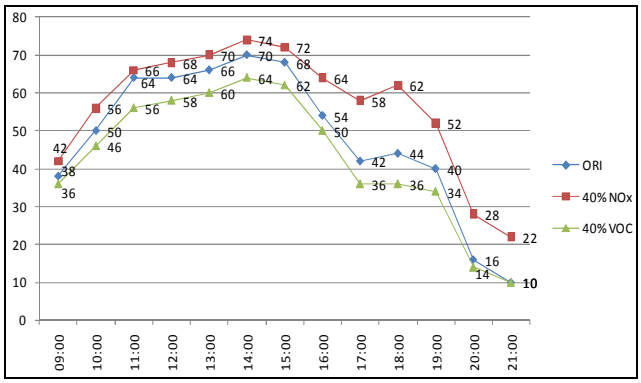

Fig 14. Ozone response to new emission scenarios

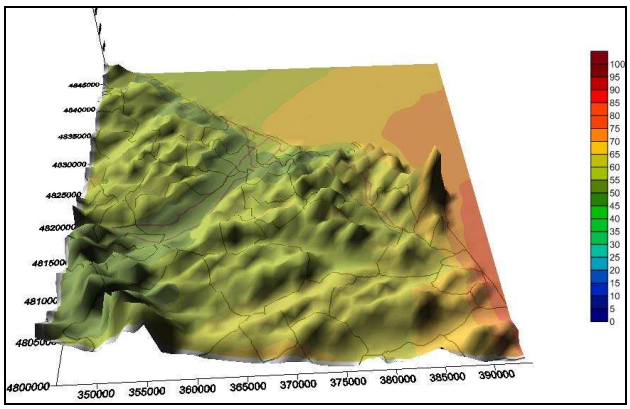

Fig 15. August 28, 2006 - 11 AM: ozone concentrations at ground level (μg/m^3), original emission scenario

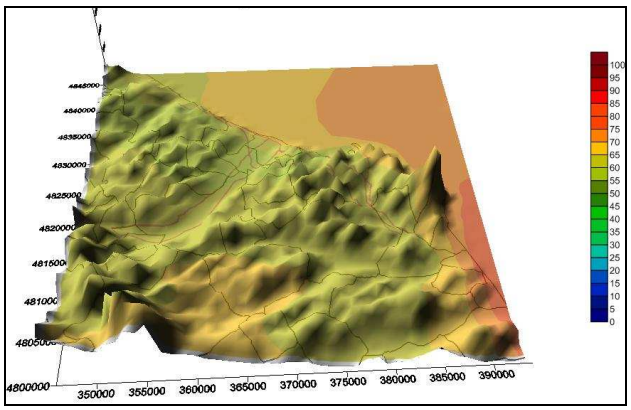

Fig 16. August 28, 2006 - 11 AM - Ozone concentrations at ground level (μg/m^3), with a 40% reduction of NOx, become higher

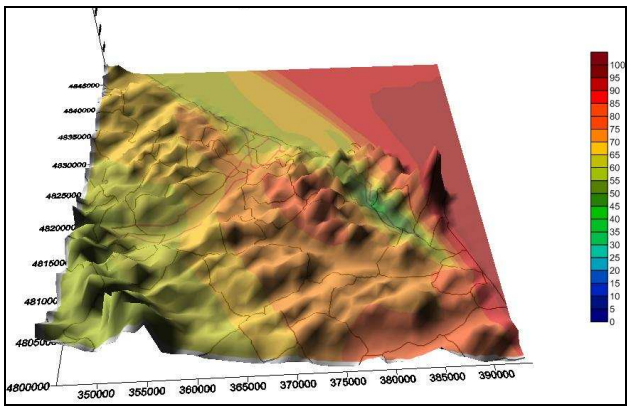

Fig 19. August 28, 2006 - 6 PM - Ozone concentrations at ground level (μg/m^3), with a 40% reduction of NOx, become higher

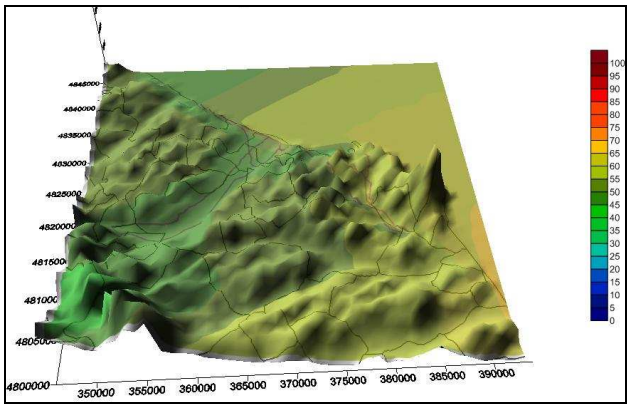

Fig 17. August 28, 2006 - 11 AM - Ozone concentrations at ground level (μg/m^3), with a 40% reduction of VOC, become lower

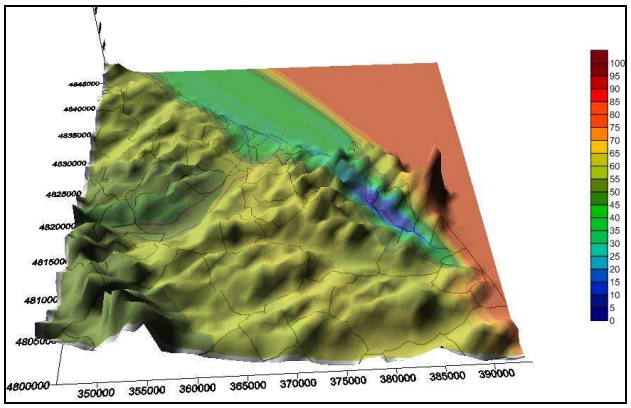

Fig 20. August 28, 2006 - 6 PM- Ozone concentrations at ground level (μg/m^3), with a 40% reduction of VOC, become lower

9. Ozone control strategies

Information about ozone condition of formation could be very useful in tuning ozone control strategies to reach acceptable air quality and to avoid ozone episodes. For instance, in a VOC-limited situation, reducing the NOx emission will result in an increased ozone concentration since more NO_2 will be available to reform ozone due to a reduced efficiency of reaction (1). Just a small amount will be transformed into HNO_3.

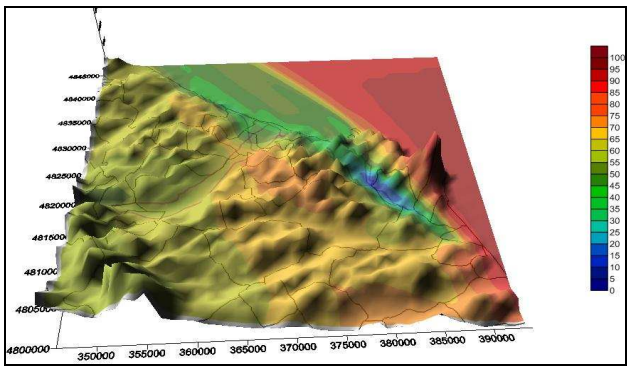

Fig 18. August 28, 2006 - 6 PM: ozone concentrations at ground level (μg/m^3), original emission scenario

To investigate how changes in emission scenarios will influence ozone behavior in the area, we carried out several other simulations through speculative reductions of emissions. Fig14 shows the ozone response in two different scenarios with 40% reduction of NOx or of VOC in emission inventory. As we can see, a 40% reduction of VOC emissions will result in lower ozone concentrations during while reduced NOx emissions, will trigger an increase of the ozone concentration as previously noticed in northern Italy (Gabusi and Volta 2005).

Fig 15 to 20 show the ozone concentrations in these three different emission scenarios at 11AM and 6PM. The blue area on Fig.18 and 20 covers the main Adriatic highway, which is the highest source of NOx emissions that locally decrease the ozone concentrations (Luria *et al.* 2008).

10. Conclusions

We determined a VOC-limited situation in the first part of the morning and, in this condition, a reduction in NOx emission will increase ozone concentrations. The transition point is at about 12:30 AM. Whenever the NOx-limited situation persists during the night, this inhibits the ozone destruction processes and only the new VOC-limited condition, in the following early morning, is able to trigger it.

Fig 21 reassumes an entire ozone day-cycle at "Falconara Scuola" site. The classical VOC/NOx curve has been plotted, based on monitored values, together with local ozone concentrations. A VOC-limited situation (VOC/NOx<5.5) happens in the first part of the morning followed by a NOx-limited situation (VOC/NOx>5.5) that keeps going during the night. In this case, the VOC-limited situation happens before the one predicted by the OSAT because of the different VOC/NOx ratio given in input to the model. The higher this ratio is, the earlier the transition occurs.

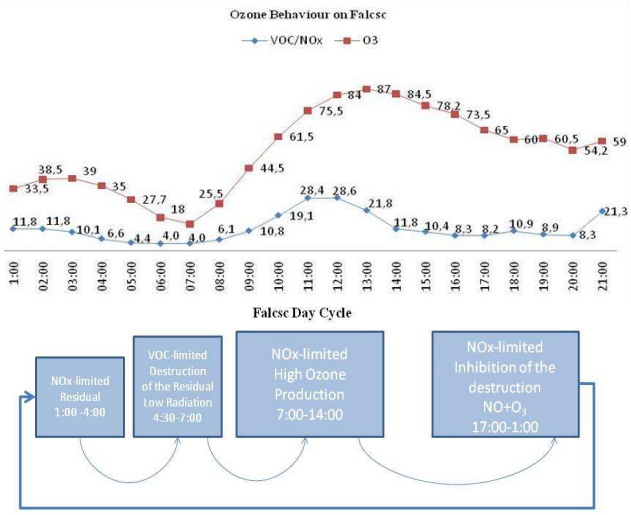

Fig 21. Ozone Day Cycles at "Falconara Scuola"

As a further proof, detailed analysis carried out on the "High Environmental Risk Area" inside the G3 grid, has showed a more efficient ozone depletion over the main Highway, an area where NOx emissions are very high. The rest of the area retains high Ozone concentrations that persist up to the next morning shift when ozone depletion finally happens.

Based on such evidence, policy makers must be aware that stopping industrial activities and/or private cars, with the aim of reducing ozone levels, may lead to exacerbation of phenomena and even to ozone episodes. In fact, reducing such human activities may lead to a further increase of VOC/NOx ratio since most VOC are due to diffuse emissions while NOx are mostly stack and exhaust-pipe emissions.

References

Barker, J. R. 1995. *Progress and problems in atmospheric chemistry*. World Scientific, USA. 941.

Cody, R. P.; Weisel, C. P.; Birnbaum, G.; Lioy, J. 1992. The effects of ozone associated with summer time photochemical smog on the frequency of asthma visits to hospital emergency departments. *Environmental Research*, 58: 184–194.

Dunker, A.; Yarwood, G.; Portmann, J.; Wilson, G. M. 2002. Comparison of Source Apportionment and Source Sensitivity of Ozone in a Three-Dimensional Air Quality Model. *Env. Science & Techn*., 36(13): 2953–2964.

EMEP. 2003. *Transboundary Acidification, Eutrophication and Ground Level Ozone in Europe*. 56.

Gabusi, V.; Volta, M. 2005. Seasonal modelling assessment of ozone sensitivity to precursors in northern Italy. *Atmospheric Environment* 39: 2795–2804.

Gery, M. W.; Whitten, G. Z.; Killus, J. P.; Dodge, M.C. 1989. A Photochemical Kinetics Mechanism for Urban and Regional Scale Computer Modeling. *J. Geophys. Res.*, 94: 925–956.

Luria, M.; Valente, R. J.; Bairai, S.; Parkhurst, W. J.; Tanner, R. L. 2008. Nighttime chemistry in the Houston urban plume. *Atmospheric Environment* 42: 7544–7552.

Morris, R. E.; Yarwood, G.; Emery, C. A.; Wilson, G. M. 2001. Recent Advances in CAMx Air Quality Modeling, In *Proc. of Second Conference on Air Pollution Modelling and Simulation, Champs-sur-Marne*. 79–92.

Seinfeld, J.; Spyros, N. 2006. *Atmospheric chemistry and physics: From Air Pollution to Climate Change.* John Wiley & Sons, INC. Hoboken, New Jersey. 1248. ISBN 0-471-17816-0.

Sillman, S. 1995. The use of NOy, H_2O_2, and HNO_3 as indicators for ozone-NOx-hydrocarbon sensitivity in urban locations. *Journal of Geophysical Research*, 100: 14175–14188.

Sillman, S.; He, D. 2002. Some theoretical results concerning O3-NOx-VOC chemistry and NOx-VOC indicators. *Journal of Geophysical Research*, 107 (D22): 4659–4671.

Sillman, S.; He, D.; Cardelino, C.; Imhoff, R. E. 1997. The use of photochemical indicators to evaluate ozone-NOx- Hydrocarbon sensitivity: Case studies from Atlanta. New York, and Los Angeles. *Journal of the Air and Waste Management Association*, 47: 1030–1040.

Sillman, S.; Logan, J. A.; Wofsy, S. C. 1990. The sensitivity of ozone to nitrogen oxides and hydrocarbons in regional ozone episodes. *Journal of Geophysical Research*, 95: 1837–1851.

Walko, R. L.; Tremback, C. J. 2006. *RAMS, The Regional Atmospheric Modeling System, Version 6.0*, ATMET.